Propagation of instability in dielectric elastomers

Jinxiong Zhou [a,b], Wei Hong [a], Xuanhe Zhao [a], Zhiqian Zhang [c], Zhigang Suo [a,*]

[a] *School of Engineering and Applied Sciences, Harvard University, Cambridge, MA 02138, USA*
[b] *MOE Key Laboratory for Strength and Vibration, School of Aerospace, Xi'an Jiaotong University,*
Xi'an 710049, People's Republic of China
[c] *Faculty of Science and Technology, Keio University, Yokohama 223-8522, Japan*

Abstract

When an electric voltage is applied across the thickness of a thin layer of an dielectric elastomer, the layer reduces its thickness and expands its area. This electrically induced deformation can be rapid and large, and is potentially useful as soft actuators in diverse technologies. Recent experimental and theoretical studies have shown that, when the voltage exceeds some critical value, the homogenous deformation of the layer becomes unstable, and the layer deforms into a mixture of thin and thick regions. Subsequently, as more electric charge is applied, the thin regions enlarge at the expense of the thick regions. On the basis of a recently formulated nonlinear field theory, this paper develops a meshfree method to simulate numerically this instability.
© 2007 Elsevier Ltd. All rights reserved.

1. Introduction

Dielectric elastomers are being used to develop lightweight, low-cost, and compliant actuators. Potential applications include artificial muscles for robots, micro air vehicles and medical devices (e.g., Sugiyama and Hirai, 2006; Kofod et al., 2007; Chu et al., 2006; Pelrine et al., 2000; Zhang et al., 2002; Galler et al., 2006; Tolksdorf et al., 2001). Partly stimulated by these technological potentials, there has been renewed interest in developing nonlinear field theory of elastic dielectrics (e.g., Dorfmann and Ogden, 2005; McMeeking and Landis, 2005; Suo et al., 2007; Vu et al., 2007). For example, Suo et al. (2007) have abandoned the troublesome notions of electric body force and Maxwell stress, and formulated a theory consisting of decoupled, linear partial differential equations and boundary conditions, with nonlinear electromechanical coupling fully captured by a free-energy function.

On the basis of this theory, the present paper develops a meshfree method to simulate a phenomenon observed in electrically induced deformation. It was Stark and Garton (1955) who first reported that the

---

* Corresponding author. Tel.: +1 617 4953789; fax: +1 617 4960601.
  E-mail address: suo@deas.harvard.edu (Z. Suo).

breakdown fields of polymers reduced when the polymers became soft at elevated temperatures. The phenomenon is understood as follows. The electric voltage is applied between the electrodes on the top and the bottom surfaces of a thin layer of a polymer. As the electric field increases, the polymer thins down, so that the same voltage will induce an even higher electric field. This positive feedback results in a mode of instability, known as electromechanical instability or pull-in instability, which causes the polymer to reduce the thickness drastically, often leading to electrical breakdown. This instability has been recognized as a failure mode of the insulators for power transmission cables (Dissado and Fothergill, 1992).

A different experimental manifestation of the electromechanical instability has been reported recently (Plante and Dubowsky, 2006). Under certain conditions, an electric voltage can deform a layer of a dielectric elastomer into a mixture of two regions, one being flat and the other wrinkled (Fig. 1). In the experiment, the electrodes on the top and the bottom surfaces of the dielectric layer were made of conducting grease, which applied a uniform electric potential to the elastomer without constraining its deformation.

This experimental observation has been interpreted as follows (Zhao et al., in press). Fig. 2a sketches the experimental observation with a top view and cross sectional view. Fig. 2b sketches the relation between the electric voltage Φ applied between the top and the bottom electrodes and the magnitude of the electric charge Q on either electrode. When the voltage is small, the elastomer deforms slightly, and the charge increases with the voltage approximately linearly. As the voltage increases, the elastomer thins down significantly, and a small increase in the voltage adds a large amount of charge on either electrode. Consequently, the voltage may reach a peak; as more charge is added on the electrodes, the elastomer thins down further, and the voltage needed to maintain the charge drops. The peak voltage corresponds to the pull-in instability. When the elastomer is thin enough, however, the large deformation may stiffen the elastomer significantly so that the voltage must increase again to thin down the elastomer further. At a given voltage, the thin state requires more charge. Consequently, as more charge is applied, the thin region enlarges at the expense of the thick region. The mixture of the two regions is in equilibrium when the electric voltage is held at a level that makes the two shaded areas in Fig. 2b equal. The thin region expands laterally more than the thick region, and wrinkles to partially relieve the elastic energy.

Fig. 1. An experimental observation of electromechanical instability (courtesy of Plante and Dubowsky). A layer of a dielectric elastomer, coated with conductive grease on top and bottom faces, is pre-stretched using a frame. An electric voltage is applied between the two electrodes. The layer deforms into a mixture of two regions, one being flat and the other wrinkled. For further experimental details see Plante and Dubowsky (2006).
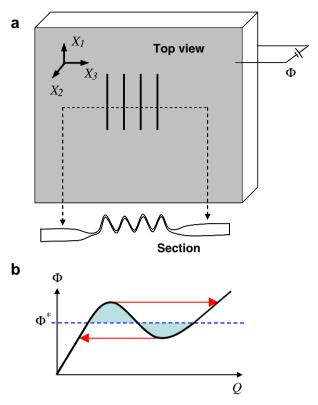
Fig. 2. (a) A schematic of an experimental observation reported by Plante and Dubowsky (2006). A thin layer of a dielectric elastomer is subject to an electric voltage across its thickness. When the voltage is small, the layer deforms homogeneously, thinning in the thickness direction and expanding in the lateral directions. When the voltage reaches a certain level, the homogeneous deformation becomes unstable, and the layer deforms into a mixture of two states, one being flat and the other wrinkled. (b) A schematic plot of the relation between the voltage applied between the two electrodes and the magnitude of the electric charge on either electrode.

The analysis of Zhao et al. (in press) assumes that the thin region and the thick region are each in a state of homogenous deformation, and neglects the constraint between the two regions. Starting with this paper, we wish to develop methods to analyze the inhomogeneous deformation. This paper is organized as follows. Section 2 summarizes the nonlinear field theory of elastic dielectrics. Section 3 describes a procedure to discretize the field equations using a meshfree method, and solve the resulting nonlinear algebraic equations using the Newton–Raphson method. Section 4 describes a material model, which we call the ideal dielectric elastomer. As a first attempt to analyze the transition between the thin and the thick states, Section 5 introduces a two-dimensional model. Section 6 reports preliminary numerical results.

2. Nonlinear field theory of elastic dielectrics

This section summarizes the nonlinear field theory of elastic dielectrics, following closely the formulation of Suo et al. (2007). Only the relations relevant to the present work are included; the reader is directed to the original paper for motivations for various definitions. We model an elastic dielectric as a continuous body of material particles. The body may extend to the entire space, but may contain interfaces between dissimilar media. Any state of the body can serve as a reference state. In the reference state, let $\mathbf{X}$ be the coordinates of a material particle, $dV(\mathbf{X})$ be an element of volume around $\mathbf{X}$, and $dA(\mathbf{X})$ be an element of an interface around $\mathbf{X}$.

In the current state at time t, the material particle $\mathbf{X}$ is at a place with coordinates $x_i = x_i(\mathbf{X}, t)$. The deformation gradient tensor is

$$F_{iJ}(\mathbf{X}, t) = \frac{\partial x_i(\mathbf{X}, t)}{\partial X_J}. \tag{1}$$

Imagine that each material particle is connected to a weight that applies a force, and the body is subject to a field of weights. In the current state, the field of weights applies force $\tilde{b}_i(\mathbf{X}, t)dV(\mathbf{X})$ on the material element of volume, and applies force $\tilde{t}_i(\mathbf{X}, t)dA(\mathbf{X})$ on the material element of an interface. Let $\xi_i(\mathbf{X})$ be a vector test function. Define the tensor of nominal stress $s_{iJ}(\mathbf{X}, t)$ such that

$$\int s_{iJ} \frac{\partial \xi_i}{\partial X_J} \, dV = \int \tilde{b}_i \xi_i \, dV + \int \tilde{t}_i \xi_i \, dA \tag{2}$$

holds true for arbitrary test function $\xi_i(\mathbf{X})$. The volume integrals extend to the volume of the body in the reference state, and the surface integral extends to the interfaces in the reference state. In the above definition, the test function $\xi_i(\mathbf{X})$ needs to have no physical interpretation and can be of any unit. In a special case, when the test function is a small, actual deformation of the body, $\delta x_i(\mathbf{X}, t)$, the right-hand side of (2) is the actual incremental work done by the field of weights. Consequently, the nominal stress is work-conjugate to the deformation gradient.

To define various electrical quantities, imagine that each material particle is connected to a battery, which maintains the electric potential of the material particle, $\Phi(\mathbf{X}, t)$, with respect to the ground. The material itself is an insulator, but the battery may pump electric charge from the ground to the material particle. In the current state at time t, define the nominal electric field by the gradient of the electric potential:

$$\tilde{E}_J(\mathbf{X}, t) = -\frac{\partial \Phi(\mathbf{X}, t)}{\partial X_J}. \tag{3}$$

Let $\tilde{q}(\mathbf{X}, t)dV(\mathbf{X})$ be the electric charge on the element of volume, and $\tilde{\omega}(\mathbf{X}, t)dA(\mathbf{X})$ be the electric charge on the element of an interface. Let $\eta(\mathbf{X})$ be a scalar test function. Define the vector of nominal electric displacement, $\tilde{D}_J(\mathbf{X}, t)$, such that the equation

$$-\int \tilde{D}_J \frac{\partial \eta}{\partial X_J} \, dV = \int \tilde{q} \eta \, dV + \int \tilde{\omega} \eta \, dA \tag{4}$$

holds true an arbitrary test function η. This definition is equally valid when we replace $\tilde{D}_I$, $\tilde{q}$ and $\tilde{\omega}$ by corresponding increments, $\delta \tilde{D}_J$, $\delta \tilde{q}$ and $\delta \tilde{\omega}$. The test function $\eta(\mathbf{X})$ needs to have no physical interpretation and can be of any unit. In a special case, when η is the actual electric potential $\Phi(\mathbf{X}, t)$, and when the increments $\delta \tilde{D}_J$, $\delta \tilde{q}$ and $\delta \tilde{\omega}$ are used, the right-hand side of (4) is the actual incremental work done by the field of batteries. Consequently, the nominal electric displacement is work-conjugate to the nominal electric field.

For an elastic dielectric, the work done by the field of weights, $\int s_{iJ} \delta F_{iJ} \, dV$, and the work done by the field of batteries, $\int \tilde{E}_J \delta \tilde{D}_J \, dV$, are stored fully in the body as the Helmholz free energy. We next localize this statement by introducing an assumption. Let $W dV(\mathbf{X})$ be the Helmholz free energy of a material element of volume. We assume that, associated with the actual changes, δF_{iJ} and $\delta \tilde{D}_J$, the free energy of the material element changes by

$$\delta W = s_{iJ} \delta F_{iJ} + \tilde{E}_J \delta \tilde{D}_J. \tag{5}$$

Define the electrical Gibbs free energy by

$$\widehat{W} = W - \tilde{E}_J \tilde{D}_J. \tag{6}$$

A combination of (5) and (6) gives that

$$\delta \widehat{W} = s_{iJ} \delta F_{iJ} - \tilde{D}_J \delta \tilde{E}_J. \tag{7}$$

Thus, an elastic dielectric is characterized by the Gibbs free energy function $\widehat{W}(\mathbf{F}, \tilde{\mathbf{E}})$. Once this function is specified, the material laws are

$$s_{iJ}(\mathbf{F}, \tilde{\mathbf{E}}) = \frac{\partial \widehat{W}(\mathbf{F}, \tilde{\mathbf{E}})}{\partial F_{iJ}}, \tag{8a}$$

$$\tilde{D}_J(\mathbf{F}, \tilde{\mathbf{E}}) = -\frac{\partial \widehat{W}(\mathbf{F}, \tilde{\mathbf{E}})}{\partial \tilde{E}_J}. \tag{8b}$$

According to definition (3), the nominal electric field $\tilde{\mathbf{E}}$ is invariant when the entire system in the current state rotates as a rigid body. According definition (1), however, the deformation gradient $\mathbf{F}$ varies when the system in the current state rotates as a rigid body. To ensure that $\widehat{W}$ is invariant under such a rigid-body rotation, following a usual practice, we invoke the right Cauchy–Green deformation tensor, $C_{IJ} = F_{kI}F_{kJ}$, and write the free energy as a function

$$\widehat{W} = \widehat{W}(\mathbf{C}, \tilde{\mathbf{E}}). \tag{9}$$

Consequently, the material laws (8) become

$$s_{iJ}(\mathbf{C}, \tilde{\mathbf{E}}) = 2F_{iL}\frac{\partial \widehat{W}(\mathbf{C}, \tilde{\mathbf{E}})}{\partial C_{JL}}, \tag{10a}$$

$$\tilde{D}_J(\mathbf{C}, \tilde{\mathbf{E}}) = -\frac{\partial \widehat{W}(\mathbf{C}, \tilde{\mathbf{E}})}{\partial \tilde{E}_J}. \tag{10b}$$

As shown in Suo et al. (2007), definitions (1)–(4) result in a set of *linear* partial deferential equations and *linear* boundary conditions, with the mechanical fields decoupled from the electrical fields. Nonlinearity and electromechanical coupling enters solely through the free-energy function $\widehat{W} = \widehat{W}(\mathbf{C}, \tilde{\mathbf{E}})$.

In numerical calculations, as well as in device applications, one often invokes small changes near a given state. Let the given state be characterized by $\mathbf{C}$ and $\tilde{\mathbf{E}}$. Associated with small changes in the deformation gradient and in the nominal electric field, δF_{iJ} and $\delta \tilde{E}_J$, the changes in the nominal stress and the nominal electric displacements are

$$\delta s_{iJ} = H_{iJkL}\delta F_{kL} - e_{iJL}\delta\tilde{E}_L, \tag{11a}$$

$$\delta \tilde{D}_J = e_{iJL}\delta F_{iL} + \varepsilon_{JL}\delta\tilde{E}_L. \tag{11b}$$

The various tangent moduli depend on the given state, and can be calculated from the Gibbs free energy:

$$H_{iJkL}(\mathbf{C}, \tilde{\mathbf{E}}) = 2\delta_{ik}\frac{\partial \widehat{W}(\mathbf{C}, \tilde{\mathbf{E}})}{\partial C_{JL}} + 4F_{iM}F_{kN}\frac{\partial \widehat{W}(\mathbf{C}, \tilde{\mathbf{E}})}{\partial C_{JM}\partial C_{LN}}, \tag{12a}$$

$$e_{iJL}(\mathbf{C}, \tilde{\mathbf{E}}) = -2F_{iM}\frac{\partial \widehat{W}(\mathbf{C}, \tilde{\mathbf{E}})}{\partial C_{JM}\partial \tilde{E}_L}, \tag{12b}$$

$$\varepsilon_{JL}(\mathbf{C}, \tilde{\mathbf{E}}) = -\frac{\partial \widehat{W}(\mathbf{C}, \tilde{\mathbf{E}})}{\partial \tilde{E}_J \partial \tilde{E}_L}. \tag{12c}$$

3. Discretization and numerical solver

In the current state at time t, interpolate the position vector $x_i(\mathbf{X}, t)$ and the electric potential $\Phi(\mathbf{X}, t)$ as

$$x_i(\mathbf{X}, t) - X_i = N_a(\mathbf{X})u_{ai}(t), \tag{13a}$$

$$\Phi(\mathbf{X}, t) = N_a(\mathbf{X})\Phi_a(t). \tag{13b}$$

The index a, as well as the index b below, is reserved for nodes; repeated a (or b) implies summation over all nodes in the body. The quantities $u_{ai}(t)$ and $\Phi_a(t)$ are the discretized displacement and electric potential associated with node a. The shape functions $N_a(\mathbf{X})$ can be constructed in several ways; we adopt a meshfree procedure; detailed implementation can be found in Belytschko et al. (1994), Liu et al. (1995) and Chen et al. (1996).

The test functions are similarly discretized:

$$\xi_i(\mathbf{X}) = N_a(\mathbf{X})\xi_{ai}, \tag{14a}$$

$$\eta(\mathbf{X}) = N_a(\mathbf{X})\eta_a, \tag{14b}$$

where ξ_{ai} and η_a are the discretized test functions associated with node a.

The discretized deformation gradient and the discretized electric potential are

$$F_{iJ}(\mathbf{X}, t) = \delta_{iJ} + \frac{\partial N_a}{\partial X_J} u_{ai}(t),$$ (15a)

$$\tilde{E}_J(\mathbf{X}, t) = -\frac{\partial N_a}{\partial X_J} \Phi_a(t).$$ (15b)

Substituting (13) and (14) into (2) and (4), and invoking the arbitrariness of the test functions, we obtain that

$$\int s_{iJ} \frac{\partial N_a}{\partial X_J} \, dV = \int \tilde{b}_i N_a \, dV + \int \tilde{t}_i N_a \, dV.$$ (16a)

$$-\int \tilde{D}_J \frac{\partial N_a}{\partial X_J} \, dV = \int \tilde{q} N_a \, dV + \int \tilde{\omega} N_a \, dV.$$ (16b)

For a given elastic dielectric, the free-energy function $\widehat{W}(\mathbf{C}, \tilde{\mathbf{E}})$ is prescribed. The material laws (10), in conjunction with the discretization (15), express the nominal stress s_{iJ} and the nominal electric displacement $\tilde{D}_J$ in terms of $u_{ai}(t)$ and $\Phi_a(t)$. Consequently, (16) is a set of nonlinear algebraic equations for $u_{ai}(t)$ and $\Phi_a(t)$.

At a given time t, we solve the nonlinear algebraic (16) using the Newton–Raphson method. Let u_{ai} and Φ_a be the values at a particular iteration. Through material laws (10), one can calculate the associated values of s_{iJ} and $\tilde{D}_J$. The increments for the iteration, δu_{ai} and $\delta \Phi_a$, are determined by a set of linear algebraic equations:

$$\left[\int H_{iJkL} \frac{\partial N_a}{\partial X_J} \frac{\partial N_b}{\partial X_L} \, dV \right] \delta u_{bk} - \left[\int e_{iJL} \frac{\partial N_a}{\partial X_J} \frac{\partial N_b}{\partial X_L} \, dV \right] \delta \Phi_b = \int \tilde{b}_i N_a \, dV + \int \tilde{t}_i N_a \, dV - \int s_{iJ} \frac{\partial N_a}{\partial X_J} \, dV,$$ (17a)

$$-\left[\int e_{kJL} \frac{\partial N_a}{\partial X_J} \frac{\partial N_b}{\partial X_L} \, dV \right] \delta u_{bk} - \left[\int \varepsilon_{JL} \frac{\partial N_a}{\partial X_J} \frac{\partial N_b}{\partial X_L} \, dV \right] \delta \Phi_b = \int \tilde{q} N_a \, dV + \int \tilde{\omega} N_a \, dV + \int \tilde{D}_J \frac{\partial N_a}{\partial X_J} \, dV.$$ (17b)

Given a close enough initial guess, the Newton–Raphson method has a relatively fast convergence rate. To automate the process of making good guesses, the usual approach is to combine the iteration with an incremental scheme. One divides the external load into a number of increments, uses the reference state as the initial guess for the first increment, iterates within each increment until convergence, and uses the converged result as an initial guess for the next increment.

4. Ideal dielectric elastomers

For a given elastic dielectric, the material laws are fully specified by the free-energy function $\widehat{W}(\mathbf{C}, \tilde{\mathbf{E}})$. Writing an explicit form of this function for any real material is a challenging task. For many dielectric elastomers, experiments seem to suggest that (a) the true electric displacement is approximately linear in the true electric field, $\mathbf{D} = \varepsilon \mathbf{E}$, and (b) the permittivity ε is approximately independent of the state of deformation (Pelrine et al., 1998, 2000; Kofod and Sommer-Larsen, 2005; Plante and Dubowsky, 2006). These observations may be interpreted using a molecular picture. When molecular groups in an elastomer can polarize nearly as freely as in liquids, e.g., when the degree of crosslink is low and the deformation is well before individual molecular chains are fully extended, the dielectric behavior of the elastomer is expected to be liquid-like. The linearity simply suggests that the applied electric field is still too low to perfectly align polar groups (if there are any) to saturate polarization.

Let $W_0(\mathbf{C})$ be the free-energy function of the elastomer in the absence of the electric field. For the ideal dielectric elastomer, the dielectric energy per unit volume is $\varepsilon E^2 / 2$. Recall that the true electric field relates to the nominal electric field as $\tilde{E}_J = F_{iJ} E_i$, so that $E^2 = C_{IJ}^{-1} \tilde{E}_I \tilde{E}_J$, where C_{IJ}^{-1} are the components of the tensor $\mathbf{C}^{-1}$. Following Zhao et al. (in press), we define an *ideal dielectric elastomer* by writing the free energy as the sum of the elastic energy and the dielectric energy:

$$\widehat{W}(\mathbf{C}, \tilde{\mathbf{E}}) = W_0(\mathbf{C}) - \frac{1}{2} \varepsilon C_{IJ}^{-1} \tilde{E}_I \tilde{E}_J.$$ (18)

While it will be interesting to investigate how well the ideal dielectric elastomer represents a real one, in this paper we will use the ideal dielectric elastomer to develop the theory.

The elastomer is taken to be incompressible. We adopt a series expression developed by Arruda and Boyce (1993):

$$W_0 = \mu \left[\frac{1}{2}(I_1 - 3) + \frac{1}{20N}\left(I_1^2 - 9\right) + \frac{11}{1050N^2}\left(I_1^3 - 27\right) + \ldots \right], \tag{19}$$

where μ is the small-strain shear modulus, $I_1 = C_{KK}$, and N is the number of rigid molecular segments in a polymer chain between crosslinks.

Inserting (18) into (10), we obtain the material laws:

$$s_{iJ} = 2\frac{\mathrm{d}W_0}{\mathrm{d}I_1}F_{iJ} - pF_{Ji}^{-1} + \varepsilon\tilde{E}_L\tilde{E}_K F_{Li}^{-1} C_{KJ}^{-1}, \tag{20a}$$

$$\tilde{D}_J = \varepsilon\tilde{E}_L C_{JL}^{-1}, \tag{20b}$$

where p is a penalty coefficient introduced to enforce incompressibility (e.g., Holzapfel, 2001, p. 222).

5. A two-dimensional approximation

The above formulation is valid for three-dimensional fields. While the instability reported by Plante and Dubowsky (2006) involves three-dimensional deformation, in this first numerical treatment of this instability, we will formulate an approximate two-dimensional model. Let X_3 be the direction along the wave vector of the wrinkles. In this direction, we expect that the nominal stress s_{33} is nearly relieved by the wrinkles. Imagine a slice of the thin film cut along a wrinkle, the slice should be in a generalized plane-stress state rather than a plane-strain state. In the approximate model, we set $s_{33} = 0$. We will study the field in a (X_1, X_2) plane, and neglect $F_{\alpha 3}$, $F_{3\Gamma}$ and $\tilde{E}_3$; the Greek subscripts run from 1 to 2. We do allow the stretch along the x_3 direction, $F_{33} = \lambda_3$. The incompressibility of the elastomer relates λ_3 to the in-plane deformation as

$$\lambda_3 = \frac{1}{\sqrt{C_{11}C_{22} - C_{12}^2}}. \tag{21}$$

The above two-dimensional approximation is rigorous when the material undergoes a homogenous deformation and is stress-free in the X_3 direction. For situations with coexistent states of different thicknesses, error occurs in the transition regions between two phases; a more rigorous model will be formulated in a subsequent paper.

Substituting $s_{33} = 0$ into (20a), we find that

$$p = 2\lambda_3^2 \frac{\mathrm{d}W_0}{\mathrm{d}I_1}. \tag{22}$$

We can rewrite the in-plane components of the nominal stress tensor as

$$s_{\alpha\Gamma} = 2\frac{\mathrm{d}W_0}{\mathrm{d}I_1}\left(F_{\alpha\Gamma} - \lambda_3^2 F_{\Gamma\alpha}^{-1}\right) + \varepsilon\tilde{E}_\Lambda\tilde{E}_\Theta F_{\Lambda\alpha}^{-1} C_{\Theta\Gamma}^{-1}. \tag{23}$$

The tangent moduli can be calculated from

$$4\frac{\partial\widehat{W}(\mathbf{C}, \tilde{\mathbf{E}})}{\partial C_{\Gamma\Lambda}\partial C_{\Theta\Xi}} = 4\left[\frac{\mathrm{d}^2 W_0}{\mathrm{d}I^2}\left(\delta_{\Gamma\Lambda} - \lambda_3^2 C_{\Gamma\Lambda}^{-1}\right)\left(\delta_{\Theta\Xi} - \lambda_3^2 C_{\Theta\Xi}^{-1}\right) + \frac{\lambda_3^2}{2}\frac{\mathrm{d}W_0}{\mathrm{d}I}\left(2C_{\Gamma\Lambda}^{-1}C_{\Theta\Xi}^{-1} + C_{\Gamma\Theta}^{-1}C_{\Lambda\Xi}^{-1} + C_{\Gamma\Xi}^{-1}C_{\Lambda\Theta}^{-1}\right)\right]$$
$$- \varepsilon\tilde{E}_\Pi\tilde{E}_\Sigma\left[C_{\Lambda\Pi}^{-1}\left(C_{\Gamma\Theta}^{-1}C_{\Xi\Sigma}^{-1} + C_{\Gamma\Xi}^{-1}C_{\Theta\Sigma}^{-1}\right) + C_{\Gamma\Sigma}^{-1}\left(C_{\Lambda\Xi}^{-1}C_{\Theta\Pi}^{-1} + C_{\Lambda\Theta}^{-1}C_{\Xi\Pi}^{-1}\right)\right] \tag{24}$$

$$2\frac{\partial\widehat{W}(\mathbf{C}, \tilde{\mathbf{E}})}{\partial C_{\Gamma\Lambda}\partial\tilde{E}_\Theta} = \varepsilon\tilde{E}_\Xi\left(C_{\Gamma\Theta}^{-1}C_{\Lambda\Xi}^{-1} + C_{\Gamma\Xi}^{-1}C_{\Lambda\Theta}^{-1}\right). \tag{25}$$

6. Numerical results and discussion

As a numerical example, consider a thin layer of a dielectric elastomer sandwiched between two compliant electrodes. A voltage Φ is applied between the two electrodes, and no external forces are applied. When the voltage is small, the deformation in the layer is homogenous. When the voltage reaches a critical value, however, the homogenous deformation is unstable, and gives way to inhomogeneous deformation. Zhao et al. (in press) have analyzed the stability of the homogenous deformation. Here, we will use our numerical procedure to recover the homogenous deformation, and analyze the inhomogeneous deformation.

We first summarize the basic results of the homogenous deformation. Let H the thickness of the undeformed elastomer, and λH be the thickness of the deformed elastomer. In the current state, the nominal electric field is $\tilde{E} = \Phi/H$, and the true electric field is $E = \Phi/(\lambda H) = \tilde{E}/\lambda$. Due to incompressibility, the stretch in a direction normal to the thickness is $\lambda^{-1/2}$. Consequently, $I_1 = \lambda^2 + 2\lambda^{-1}$, and the free-energy function of the elastomer is

$$\widehat{W}(\lambda, \tilde{E}) = W_0(\lambda) - \frac{\varepsilon}{2}\left(\frac{\tilde{E}}{\lambda}\right)^2, \tag{26}$$

where $W_0(\lambda)$ is obtained by inserting $I_1 = \lambda^2 + 2\lambda^{-1}$ into (19). The nominal stress in the thickness direction is

$$s = \frac{\partial \widehat{W}(\lambda, \tilde{E})}{\partial \lambda} = \frac{\mathrm{d}W_0(\lambda)}{\mathrm{d}\lambda} + \varepsilon\tilde{E}^2\lambda^{-3}. \tag{27}$$

The nominal electric displacement is

$$\tilde{D} = -\frac{\partial \widehat{W}(\lambda, \tilde{E})}{\partial \tilde{E}} = \varepsilon\tilde{E}\lambda^{-2}. \tag{28}$$

Because no external force is applied, $s = 0$, and (27) and (28) may be written as

$$\tilde{E} = \sqrt{-\frac{\lambda^3 \mathrm{d}W_0(\lambda)}{\varepsilon \mathrm{d}\lambda}}, \quad \tilde{D} = \sqrt{-\frac{\varepsilon \mathrm{d}W_0(\lambda)}{\lambda \mathrm{d}\lambda}}. \tag{29}$$

This pair of equations define the relation between $\tilde{D}$ and $\tilde{E}$, with λ as a parameter.

We next use our meshfree code to recover this homogeneous deformation. For the homogenous deformation, the size of the block is unimportant, and is set to be $L \times H$ with the aspect ratio $L/H = 1$ (Fig. 3), discretized using 132 nodes. Fig. 4 compares the calculated voltage–charge relation with (29). The voltage is
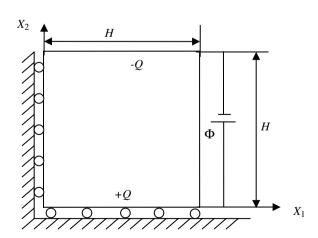

Fig. 3. A schematic of the computational model. A square block ($H \times H$) of dielectric elastomer, with two sides constrained frictionlessly, and two compliant electrodes deposited on the top and bottom sides. A voltage Φ is applied between the two electrodes, and induces charge $+Q$ on one electrode, and $-Q$ on the other electrode.

normalized as $\Phi/\left(H\sqrt{\varepsilon/\mu}\right)$, and the charge is normalized as $Q/\left(L\sqrt{\varepsilon\mu}\right)$. The only dimensionless parameter in the problem is N in (19). The numerical results agree well with the analytical solutions, even when a homogenous deformation is unstable, i.e. the parts in the plot with negative slopes. The exception is when $N \to \infty$, where the instability is so catastrophic that even a smallest numerical error makes the Newton–Raphson iteration diverge.

We finally use the meshfree code to simulate inhomogeneous deformation. The size of the block is now set as $L \times H$, with the aspect ratio $L/H = 8$ (Fig. 5). The block is discretized using 246 nodes. The material parameter is taken to be $N = 2.8$. To introduce an initial imperfection, we modify the vertical coordinates of three nodes on the top surface, lowering the middle node by $0.002H$, and lowering the two neighboring nodes by $0.001H$. We use the total charge Q on the top electrode to control the incremental loading and unloading process.
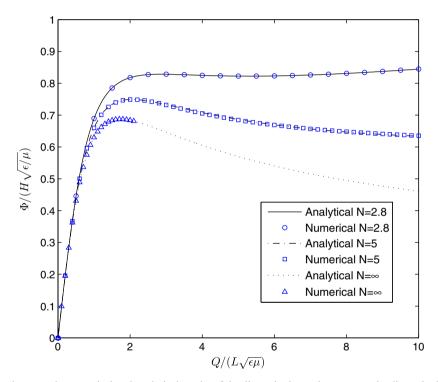

Fig. 4. A comparison between the numerical and analytical results of the dimensionless voltage versus the dimensionless charge. No initial imperfection is introduced. For Arruda–Boyce materials ($N = 2.8$ and 5), the numerical results agree well with the analytical solutions, even in the region when the homogenous solution is unstable. For neo-Hookean material ($N = \infty$), in the region when the homogenous solution is unstable, the Newton–Raphson iteration fails to converge.
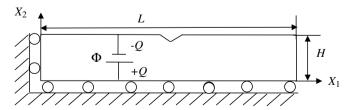

Fig. 5. A schematic of the computational model of a rectangular block ($L \times H$) of dielectric elastomer, with a small imperfection. (The size of the imperfection is exaggerated for visual clarity.) The left and bottom sides are constrained frictionlessly. Two compliant electrodes are deposited on the top and bottom surfaces. A voltage Φ is applied between the two electrodes, and induces charge $+Q$ on one electrode, and $-Q$ on the other electrode.

Four stages of deformation can be observed, noted as B–E in Figs. 6 and 7. (The stage A in Fig. 7 denotes the reference state.) In stage B, the elastomer is uniformly thinned, all the way until it reaches some point near the critical voltage, when the homogenous deformation is unstable and a local region thins down preferentially. In stages C and D, the elastomer deforms into a mixture of two states. The voltage keeps constant, but as electric charge is pumped onto the electrodes, the thin region grows at the expense of the thick region. From stage C to stage D, instability propagates in the elastomer. In these stage, the numerical solution deviates from the analytical homogenous solution, shown as a horizontal line in Fig. 6. A discontinuity in voltage near point D can be seen on Fig. 6. The phenomenon can be understood as follows. Although the coexistence
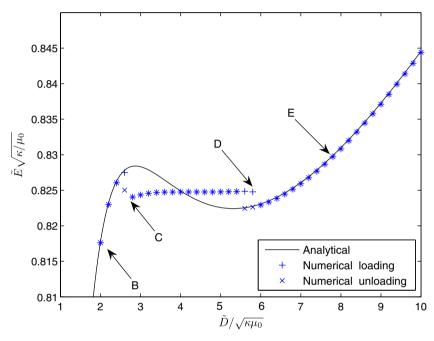

Fig. 6. Numerical and analytical results of the dimensionless voltage as a function of the dimensionless charge. An Arruda–Boyce material with $N = 2.8$ is assumed. Stage A denotes the reference state and is not shown here. States B and E represent two homogeneous states while C and D are the transition states between states B and E. States C and D corresponding to inhomogeneous deformations and can not be obtained by analytical method.
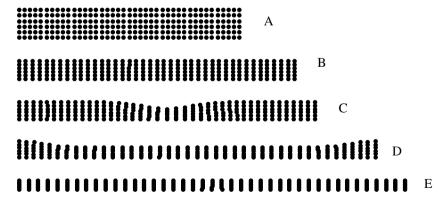

Fig. 7. A sequence of deformation as obtained by numerical simulation. A is the reference state without deformation, stages B and E are in the conditions when a homogenous solution is stable, and the elastomer deforms uniformly. In stages C and D, two states of different thicknesses coexist. From stage C to stage D, instability propagates in elastomer. When the charge on the electrodes increases, the thinner region grows at the expense of the thicker region until the thicker region is exhausted. When the charge decreases, the thinner region shrinks until it reaches the uniform thicker state.

of the two states of different thicknesses is having a lower energy than one of the states, there is always a transition region of finite width that costs extra energy in between the two states. When the thinner state propagates to some point close to the edge, there will be no space for the thicker state to exist. Comparing to that of a uniform thin state, the energy is higher for a thin state to exist with a transition region, but without the thick state. As a result, the film snaps down at this point, from the combination of a thin state with an edge of transition region to a uniform thin state. The deformation becomes homogenous when the thick region is exhausted. In stage E, the material deforms uniformly again, but with a much thinner thickness. When we unload the material by withdrawing electric charge from the electrodes, the material relaxes almost along the same route, except for the position of critical points.

7. Concluding remarks

On the basis of a recently formulated nonlinear field theory of elastic dielectrics, we have developed a meshfree code to simulate electrically induced finite deformation in elastomers. The procedure is demonstrated for the ideal dielectric elastomer, subject to two-dimensional approximations, using meshfree method. We apply the numerical method to simulate a layer subject to a voltage. When the voltage is small, the deformation of the layer is homogenous. When the voltage reaches a certain value, deformation becomes inhomogeneous, with coexistent thin and thick state. At a constant voltage, as the battery pumps more charge to the two electrodes, the thin region expands at the expense of the thick region. The general numerical procedure has the clear potential to be extended to simulate more complex modes of deformation in dielectric elastomers.

References

Arruda, E.M., Boyce, M.C., 1993. A three-dimensional constitutive model for the large stretch behavior of rubber elastic materials. J. Mech. Phys. Solids 41, 389–412.

Belytschko, T., Lu, Y.Y., Gu, L., 1994. Element-free Galerkin methods. Int. J. Numer. Meth. Eng. 37, 229–256.

Chen, J.S., Pan, C., Wu, C.T., Liu, W.K., 1996. Reproducing kernel particle methods for large deformation analysis of nonlinear structures. Comput. Meth. Appl. Mech. Eng. 139, 195–229.

Chu, B.J., Zhou, X., Ren, K.L., Neese, B., Lin, M.R., Wang, Q., Bauer, F., Zhang, Q.M., 2006. A dielectric polymer with high electric energy density and fast discharge speed. Science 5785, 334–336.

Dissado, L.A., Fothergill, J.C., 1992. Electrical Degradation and Breakdown in Polymers. Peter Peregrinus Ltd, London.

Dorfmann, A., Ogden, R.W., 2005. Nonlinear electroelasticity. Acta Mech. 174, 167–183.

Galler, N., Ditlbacher, H., Steinberger, B., 2006. Electrically actuated elastomers for electo-optical modulators. Appl. Phys. B 85, 7–10.

Holzapfel, G.A., 2001. Nonlinear Solid Mechanics. Wiley, New York.

Kofod, G., Sommer-Larsen, P., 2005. Silicon dielectric elastomer actuators: finite elasticity model of actuation. Sensor Actuator A 122, 273–283.

Kofod, G., Wirges, W., Paajanen, M., Bauer, S., 2007. Energy minimization for self-organized structure formation and actuation. Appl. Phys. Lett. 90, 081916.

Liu, W.K., Jun, S., Zhang, Y.F., 1995. Reproducing kernel particle methods. Int. J. Numer. Meth. Eng. 20, 1081–1106.

McMeeking, R.M., Landis, C.M., 2005. Electrostatic forces and stored energy for deformable dielectric materials. J. Appl. Mech. 72, 581–590.

Plante, J.S., Dubowsky, S., 2006. Large-scale failure modes of dielectric elastomer actuators. Int. J. Solid Struct. 43, 7727–7751.

Pelrine, R., Kornbluh, R., Joseph, J., 1998. Electrostriction of polymer dielectrics with compliant electrodes as a means of actuation. Sensor Actuator A: Phys. 64, 77–85.

Pelrine, R., Kornbluh, R., Pei, Q., Joseph, J., 2000. High-speed electrically actuated elastomers with strain greater than 100%. Science 287, 836–839.

Stark, K.H., Garton, C.G., 1955. Electric strength of irradiated polythene. Nature 176, 1225–1226.

Sugiyama, Y., Hirai, S., 2006. Crawling and jumping by a deformable robot. Int. J. Robotic Res. 25, 603–620.

Suo, Z., Zhao, X., Greene, W.H., 2007. A nonlinear field theory of deformable dielectrics. J. Mech. Phys. Solids, doi:10.1016/j.jmps.2007.05.021.

Tolksdorf, C., Gebhard, E., Zentel, R., Kruger, P., Losche, M., Kremer, F., 2001. Giant lateral electrostriction in ferroelectric liquid-crystalline elastomers. Nature 410, 447–450.

Vu, D.K., Steinmann, P., Possart, G., 2007. Numerical modelling of non-linear electroelasticity. Int. J. Numer. Meth. Eng. 70, 685–704.

Zhang, Q.M., Li, H., Poh, M., Xia, F., Cheng, Z.Y., Xu, H., Huang, C., 2002. An all-organic composite actuator material with a high dielectric constant. Nature 419, 284–287.

Zhao, X., Hong, W., Suo, Z., in press. Electromechanical hysteresis and coexistent states in dielectric elastomers. Phys. Rev. B, http://imechanica.org/node/1283.